

# LncRNA LINC00961 regulates endothelial-mesenchymal transition via the PTEN-PI3K-AKT pathway

JIN-XING HU<sup>1</sup>, ZE-QI ZHENG<sup>1</sup>, TING KANG<sup>1</sup>, WEI QIAN<sup>1</sup>, SHAN-HUA HUANG<sup>1</sup> and BIN-GONG LI<sup>1,2</sup>

<sup>1</sup>Department of Cardiology, First Affiliated Hospital, Nanchang University, Nanchang, Jiangxi 330033;

<sup>2</sup>Department of Cardiology, Qingdao Municipal Hospital, Qingdao, Shandong 266011, P.R. China

Received April 14, 2022; Accepted May 18, 2022

DOI: 10.3892/mmr.2022.12762

**Abstract.** The long noncoding RNA LINC00961 plays a crucial role in cancer and cardiovascular diseases. In the present study, the role and underlying mechanism of LINC00961 in endothelial-mesenchymal transition (EndMT) induced by transforming growth factor beta (TGF- $\beta$ ), was investigated. Human cardiac microvascular endothelial cells were transfected with LV-LINC00961 or short hairpin LINC00961 plasmids to overexpress or knock down LINC00961 in the cells, respectively. The cells were then exposed to TGF- $\beta$  in serum-free medium for 48 h to induce EndMT. Flow cytometric analysis, Cell Counting Kit-8 assay and immunofluorescence staining were performed to examine the cell apoptosis rate, assess cell viability, and identify CD31<sup>+</sup>/ $\alpha$ -SMA<sup>+</sup> double-positive cells, respectively. Western blotting and reverse transcription-quantitative polymerase chain reaction were used to evaluate protein and mRNA expression, respectively. Injury to endothelial cells and EndMT was induced by TGF- $\beta$  in a time-dependent manner. LINC00961 overexpression promoted injury and EndMT, whereas LINC00961 knockdown had the opposite effects. Knockdown of LINC00961 attenuated EndMT and injury to endothelial cells induced by TGF- $\beta$  via the PTEN-PI3K-AKT pathway. Inhibition of LINC00961 expression may prevent the occurrence of EndMT-related cardiovascular diseases, such as myocardial fibrosis and heart failure. Therefore, LINC00961

shows potential as a therapeutic target for cardiovascular diseases.

## Introduction

Acute myocardial infarction is an important and lethal cardiovascular disease characterised by a sharp decline in the coronary blood supply, and it typically develops into myocardial fibrosis (1-3). Previous studies on the regulatory mechanism of myocardial fibrosis following myocardial infarction showed that myocardial fibrosis is vital to disease progression (4,5).

Long non-coding RNAs (lncRNAs) are >200 nucleotides in length and do not have protein-coding ability. LINC00961 encodes a small polypeptide of amino acid response and is highly expressed in the heart tissue, where it regulates mTORC1 activation (6). Most researchers have focused on the ability of LINC00961 to inhibit various tumours (7-9) but recently began studying its cardiovascular effects. For example, Spencer *et al* (10) identified that LINC00961 and its encoded small polypeptide of amino acid response can regulate endothelial cell adhesion, proliferation and migration, among other processes. Liu *et al* (11) found that LINC00961, via the PI3K-AKT-GSK3 $\beta$  pathway, promoted myocardial infarction. Wu *et al* (12) demonstrated that LINC00961 contributed to coronary heart disease by regulating the function of vascular smooth muscle cells.

Markwald *et al* (13) first discovered endothelial-mesenchymal transition (EndMT) through heart formation developmental studies in 1975. EndMT plays an important role in pathophysiological processes such as myocardial ischemia-reperfusion, myocardial infarction, diabetic cardiomyopathy and fibrosis (14-17). EndMT can be induced by hypoxia and attenuated by activating AMP-activated protein kinase as well as by suppressing the mammalian target of rapamycin (mTOR) signalling pathway in human cardiac microvascular endothelial cells (HCMECs) (18-20).

Phosphatase and tensin homolog deleted on chromosome 10 (PTEN) is critical for cell growth and affects the survival and proliferation of tumour cells (21,22). PTEN is also associated with regenerative processes such as nerve injury recovery (23), cardiac ischemia (24) and wound healing (25). Yang *et al* (26) revealed that B lymphoma Mo-MLV insertion region 1 homolog aggravated myocardial fibrosis and reduced

---

*Correspondence to:* Dr Bin-Gong Li, Department of Cardiology, Qingdao Municipal Hospital, 5 Donghai Zhong Road, Qingdao, Shandong 266011, P.R. China  
E-mail: libingong08@163.com

**Abbreviations:** EndMT, endothelial-mesenchymal transition; HCMEC, human cardiac microvascular endothelial cell; lncRNA, long non-coding RNA; LV, lentivirus; PTEN, phosphatase and tensin homolog deleted on chromosome 10; RT-qPCR, reverse transcription-quantitative polymerase chain reaction; SMA,  $\alpha$ -smooth muscle actin; TGF- $\beta$ , transforming growth factor beta; VOT, VO-OHpic trihydrate

**Key words:** lncRNA, LINC00961, TGF- $\beta$ , PTEN, EndMT

cardiac function after myocardial infarction by inhibiting the PTEN-PI3K-AKT pathway.

Progress has been made in understanding the functions of LINC00961. However, whether it regulates EndMT remains unclear. In the present study, it was examined whether knock-down of LINC00961 attenuates EndMT and cell injuries by activating the PTEN-PI3K-AKT pathway.

## Materials and methods

**Cell culture, cell transfection and drug treatment.** HCMECs were obtained from ScienCell Research Laboratories, Inc. and cultured in 25-cm<sup>2</sup> cell culture flasks (Corning, Inc.) in a 5% CO<sub>2</sub> atmosphere at 37°C. The culture medium was Roswell Park Memorial Institute-1640 containing 10% fetal bovine serum (both from Gibco; Thermo Fisher Scientific, Inc.). Endothelial cells were used from passages 4 to 10 for the experiments.

Short hairpin RNA (shRNA) for LINC00961 and negative control sh-scramble were acquired from Wuhan Aspen Biotechnology Co., Ltd. The plasmid sequences were as follows: sh-LINC00961-1, 5'-AGTGCCAGGACTTCTGGACCTTCA-3'; sh-LINC00961-2, 5'-CCUCAGGGAUCCUGUUAU-3'; and sh-LINC00961-3, 5'-GCUUCUUAUUCUCCUAA-3'. Lentiviruses (LV) carrying negative control scrambled RNA and shRNA were used for transfection at the optimal multiplicity of infection value. Transfection of 5 pmol shRNA was performed using Lipofectamine<sup>®</sup> RNAiMAX Reagent (Thermo Fisher Scientific, Inc.) for 5 min at room temperature. Transfected cells were analyzed following incubation for 48 h at 37°C. The LINC00961 open reading frame (ORF) full-length cDNA clone vector (containing a restriction site) was obtained from Shanghai GenePharma Co., Ltd. The LINC00961 overexpression (LV-LINC00961) vector was prepared by double digestion of the target fragment, vector fragment acquisition, double digestion of the vector, and recovery and construction of the recombinant overexpression vector.

The cells were exposed to 10 ng/ml transforming growth factor (TGF)-β1 (Aspen Biotechnology Co., Ltd.) in serum-free medium (27) for 24, 48, 72 and 96 h to induce EndMT. The cells were then randomly divided into control, TGF-β, TGF-β + sh-LINC00961, TGF-β + sh-Scramble, TGF-β + LV-LINC00961, TGF-β + LV-Control, and TGF-β + sh-LINC00961 + VO-Ohpic trihydrate groups. VO-OHpic trihydrate (VOT, C<sub>12</sub>H<sub>15</sub>N<sub>2</sub>O<sub>11</sub>), an inhibitor of PTEN, was purchased from MedChemExpress and diluted in dimethyl sulfoxide to 35 nmol/l (28). Following the treatments, HCMECs from each group were collected by centrifugation (1,000 x g at 22°C for 3 min) for experimental analysis.

**Cell Counting Kit-8.** A 96-well plate was inoculated with the cell suspension (1x10<sup>4</sup> cells/well) and the cells were pre-cultured at room temperature in an incubator for 24 h. Next, 10 μl of Cell Counting Kit-8 solution (Beyotime Institute of Biotechnology) was added to each well; the culture plate was incubated for 2 h at 37°C, after which the absorbance was measured at 450 nm with a microplate reader (Thermo Fisher Scientific, Inc.).

Table I. Primer sequences for quantitative PCR.

Primer name	Primer sequence (5'-3')
CD31	F: ACCAAGATAGCCTCAAAGTCGG R: TAAGAAATCCTGGGCTGGGAG
VE-Cadherin	F: AAGGACATAACACCACGAAACG R: GAGATGACCACGGGTAGGAAG
α-SMA	F: CTATGCCTCTGGACGCACAAC R: CCCATCAGGCAACTCGTAACTC
FSP-1	F: GGTGTCCACCTTCCACAAGTAC R: TCCTGGGCTGCTTATCTGG
Cyclin D1	F: TCCTACTTCAAATGTGTGCAGAAG R: CATCTTAGAGGCCACGAACATG
Bcl-2	F: AGGATTGTGGCCTTCTTTGAG R: AGCCAGGAGAAATCAAACAGAG
Bax	F: TCTGAGCAGATCATGAAGACAGG R: ATCCTCTGCAGCTCCATGTTAC
AKT	F: TTCTATGGCGCTGAGATTGTGT R: GCCGTAGTCATTGTCCTCCAG
PTEN	F: TGAGAGACATTATGACACCGCC R: TTACAGTGAATTGCTGCAACATG
LINC00961	F: ATGGAACCGGCAGTGATTGG R: GCGGTCACATGAAGGTCCAG
mTOR	F: AAGCCAAGCCTTGGATTTTG R: GGACGGGTGAGGTAACAGGAT
PI3K	F: GTCCTATTGTCGTGCATGTGG R: TGGGTTCTCCCAATTCAACC
GAPDH	F: CATCATCCCTGCCTCTACTGG R: GTGGGTGTCGCTGTTGAAGTC

α-SMA, α-smooth muscle actin; FSP-1, fibroblast specific protein 1; PTEN, phosphatase and tensin homolog deleted on chromosome 10.

**Flow cytometric analysis.** An Annexin V-FITC apoptosis detection kit (Sungene Biotech) was used to assess cell apoptosis according to the manufacturer's protocol. Cells were seeded into six-well plates (1x10<sup>5</sup> cells/well) and cultured until reaching 85% confluence. After digestion, suspension and centrifugation (1,000 x g at 22°C for 3 min), the precipitate was obtained, the cells were resuspended in 300 μl of binding buffer, and 5 μl of Annexin propidium iodide was added. Annexin propidium iodide was mixed and incubated for 10 min in the dark before detection with a BD FACSAriaIII flow cytometer (BD Biosciences).

**Immunofluorescence staining.** After fixing the cells for 20 min at 4°C in 4% paraformaldehyde, the cells were washed with phosphate-buffered saline for 10 min, blocked for 1 h with 5% bovine serum albumin (Gibco; Thermo Fisher Scientific, Inc.) and incubated overnight at 4°C with the primary antibody α-smooth muscle actin (SMA) (1:5,000; cat. no. 14395-1-AP; ProteinTech Group, Inc.) or CD31 (1:500; cat. no. sc-376764, Santa Cruz Biotechnology, Inc.). After incubation for 1 h with appropriate horseradish peroxidase-conjugated goat anti-rabbit secondary antibodies

Table II. Information on primary and secondary antibodies.

Antibodies	Species	Supplier	Catalogue number	Dilution
<b>Primary</b>				
GAPDH	Rabbit	Abcam	ab37168	1:10,000
PTEN	Rabbit	Abcam	ab267787	1:2,000
p-PI3k	Rabbit	Abcam	ab182651	1:500
PI3k	Rabbit	Cell Signaling Technology, Inc.	4292	1:3,000
p-AKT	Rabbit	Cell Signaling Technology, Inc.	4060	1:1,000
AKT	Rabbit	Cell Signaling Technology, Inc.	9272	1:2,000
SPARR	Rabbit	Cell Signaling Technology, Inc.	25823	1:1,000
p-mTOR	Rabbit	Cell Signaling Technology, Inc.	5536	1:500
mTOR	Rabbit	Cell Signaling Technology, Inc.	2972	1:1,000
CD31	Mouse	Santa Cruz Biotechnology, Inc.	sc-376764	1:500
VE-Cadherin	Rabbit	Thermo Fisher Scientific, Inc.	36-1900	1:500
$\alpha$ -SMA	Rabbit	ProteinTech Group, Inc.	14395-1-AP	1:5,000
FSP-1	Rabbit	ProteinTech Group, Inc.	20886-1-AP	1:1,000
Cyclin D1	Rabbit	Cell Signaling Technology, Inc.	55506	1:1,000
Bcl-2	Rabbit	Abcam	ab59348	1:1,000
Bax	Rabbit	Cell Signaling Technology, Inc.	2772	1:2,000
<b>Secondary</b>				
HRP-goat anti-rabbit		Aspen Biotechnology Co., Ltd.	AS1107	1:10,000
HRP-goat anti-mouse		Aspen Biotechnology Co., Ltd.	AS1106	1:10,000

p-, phosphorylated;  $\alpha$ -SMA,  $\alpha$ -smooth muscle actin; FSP-1, fibroblast specific protein 1; PTEN, phosphatase and tensin homolog deleted on chromosome 10; HRP, horseradish peroxidase.

(1:10,000; cat. no. AS1107; Aspen Biotechnology Co., Ltd.) at 22°C, the cells were stained with 5  $\mu$ g/ml DAPI (Beyotime Institute of Biotechnology) for 2 min at 22°C. Fluorescence microscopy (BXMI; Olympus Corporation) was performed to visualise immunofluorescence.

**Reverse transcription quantitative (RT-q) PCR.** TRIpure Total RNA Extraction Reagent [ELK (Wuhan) Biotechnology Co., Ltd.] was used to isolate total RNA from the HCMECs. All RT-qPCR steps were conducted as previously described (20,24). Relative expression changes were calculated using the  $2^{-\Delta\Delta Cq}$  method (29), and the selected reference group was referenced as 1. The primers used in PCR are listed in Table I.

**Western blot analysis.** Sodium dodecyl sulphate-polyacrylamide gel electrophoresis (10%) was performed to separate proteins from the cells and mouse hearts. Western blot analysis was performed as previously described (20,24). Details regarding the primary and secondary antibodies used are provided in Table II.

**Statistical analysis.** All analyses were performed using Prism 9.1.2 (GraphPad Software, Inc.) and SPSS 23.0 software (IBM Corp.). Unpaired t-tests were used to compare differences between two groups. The data are presented as the means  $\pm$  standard deviation; each experiment was repeated at least three times.  $P < 0.05$  was considered to indicate a statistically significant difference.

## Results

**Injury and EndMT in HCMECs induced by TGF- $\beta$ .** As revealed in Fig. 1A, cell viability was reduced over time by TGF- $\beta$ . After 24 h of treatment with TGF- $\beta$ , cell viability in the TGF- $\beta$  group did not significantly differ from that in the control group ( $P > 0.05$ ). However, compared with the control group, the TGF- $\beta$  group exhibited significant differences in cell viability after 48, 72, and 96 h of treatment ( $P < 0.05$ ). Therefore, follow-up experiments were performed using treatment with TGF- $\beta$  for 48 h. Treatment with TGF- $\beta$  for 48 h increased the apoptotic rate of endothelial cells (Fig. 1B). It was also revealed that the mRNA and protein expression levels of  $\alpha$ -SMA and fibroblast specific protein 1 (FSP-1) were elevated, whereas those of CD31 and VE-cadherin (VE-Cad) were decreased after 48 h of TGF- $\beta$  treatment compared with the control group (Fig. 1C and D;  $P < 0.05$ ). Immunofluorescence used to assess the changes in CD31 and  $\alpha$ -SMA expression levels showed the same trends as RT-qPCR and western blotting (Fig. 1E). These results revealed that the TGF- $\beta$ -induced injury and EndMT model in HCMECs was successfully established by treatment with TGF- $\beta$  for 48 h.

**LINC00961 knockdown attenuates apoptosis induced by TGF- $\beta$  in HCMECs.** The expression of LINC00961 was suppressed in endothelial cells after transfection with the sh-LINC00961-1, sh-LINC00961-2 and sh-LINC00961-3 plasmids; the expression of LINC00961 was markedly increased using the ORF full-length cDNA clone vector.

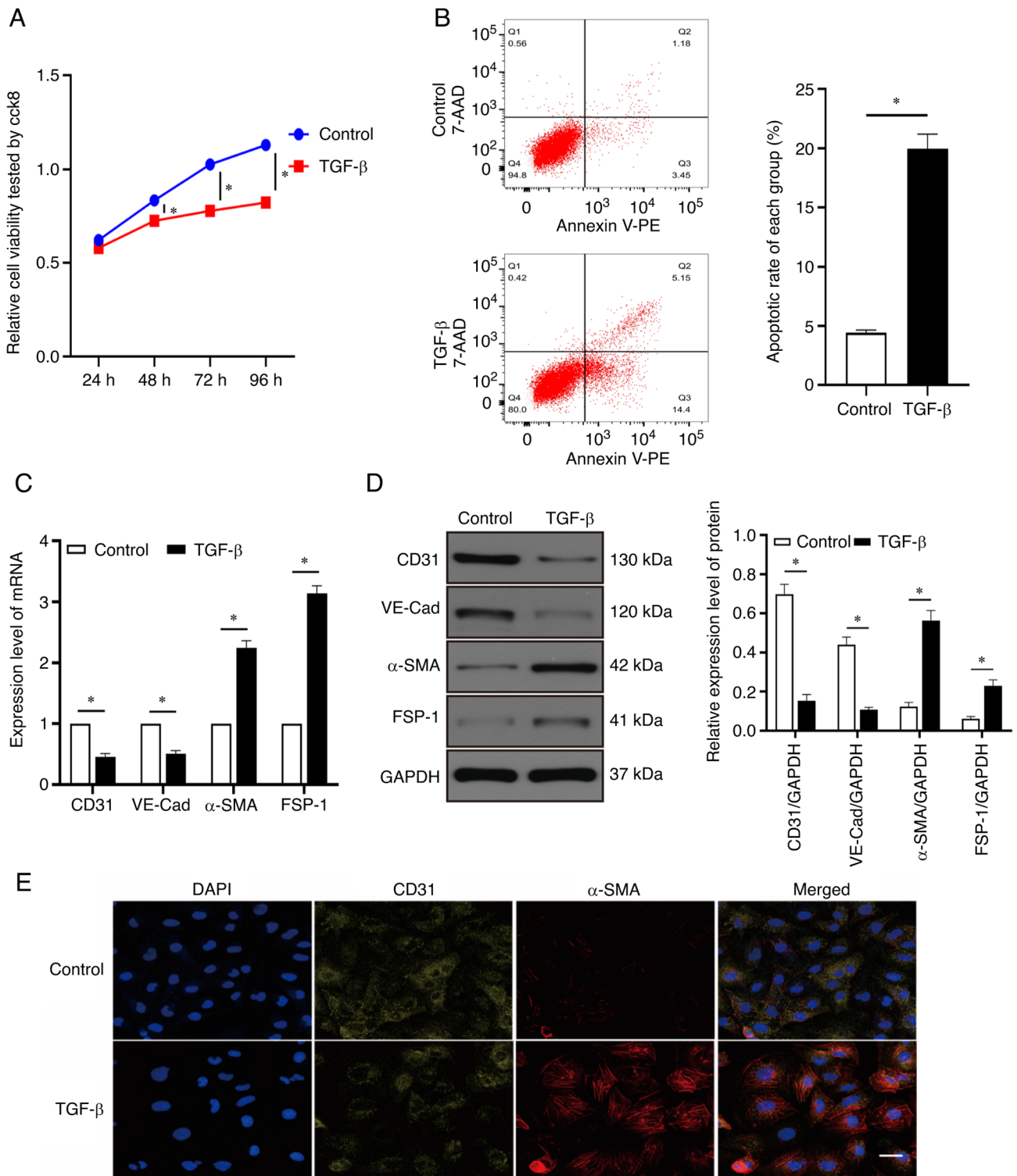


Figure 1. Injury and EndMT of HCMECs induced by TGF- $\beta$ . (A) HCMECs were treated with TGF- $\beta$  (10 ng/ml) for 24, 48, 72 and 96 h and their viability was detected using a Cell Counting Kit-8 assay. (B) Rate of cell apoptosis was evaluated using flow cytometric analysis. (C) Expression of CD31, VE-Cad,  $\alpha$ -SMA and FSP-1 mRNA was evaluated using reverse transcription-quantitative PCR. (D) Western blotting of CD31, VE-Cad,  $\alpha$ -SMA and FSP-1 protein expression. (E) Immunofluorescence staining was used to identify CD31<sup>+</sup>/ $\alpha$ -SMA<sup>+</sup> cells.  $\alpha$ -SMA (red), CD31 (green); scale bars: 50  $\mu$ m. Each experiment was repeated at least three times. ns,  $P > 0.05$ ; \* $P < 0.05$ .  $n = 5$  per group. EndMT, endothelial-mesenchymal transition; HCMECs, human cardiac microvascular endothelial cells; VE-Cad, VE cadherin;  $\alpha$ -SMA,  $\alpha$ -smooth muscle actin; ns, not significant; FSP-1, fibroblast specific protein 1.

LINC00961 levels were remarkably reduced following transfection of the sh-LINC00961-1 plasmid (Fig. 2A), and thus this plasmid was used in follow-up experiments. As revealed in Fig. 2B, LINC00961 expression was significantly increased in the TGF- $\beta$  group but was significantly reduced in the

sh-LINC00961 group compared with that in control group ( $P < 0.05$ ). LINC00961 knockdown recovered the cell viability that had been reduced by TGF- $\beta$ , whereas LINC00961 overexpression exacerbated this reduction in cell viability (Fig. 2C;  $P < 0.05$ ). Flow cytometric analysis was performed to

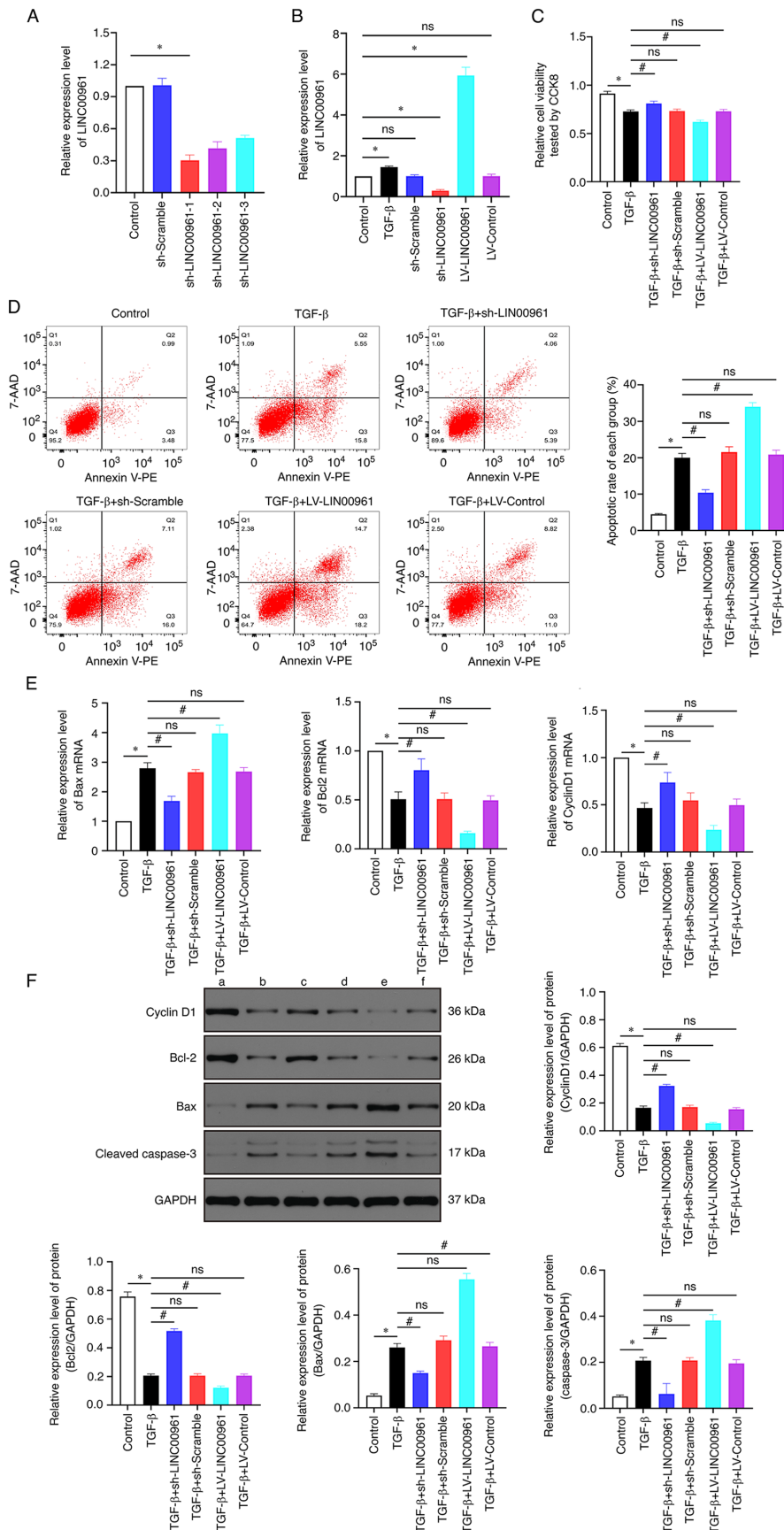


Figure 2. LINC00961 knockdown attenuates apoptosis induced by TGF-β in HCMECs. (A and B) Expression level of LINC00961 was determined using RT-qPCR. (C) Cell viability was examined using CCK-8 assay. (D) Rate of cell apoptosis was evaluated using flow cytometric analysis. (E) RT-qPCR was used to determine expression of apoptosis-related mRNA. (F) Western blotting to determine expression of apoptosis-related mRNA (a) Control, (b) TGF-β, (c) TGF-β + sh-LINC00961, (d) TGF-β + sh-Scramble, (e) TGF-β + LV-LINC00961 and (f) TGF-β + LV-Control. Each experiment was repeated at least three times. ns, P>0.05; \*P<0.05 and #P<0.05. n=5 per group. HCMECs, human cardiac microvascular endothelial cells; RT-qPCR, reverse transcription-quantitative; CCK-8, Cell Counting Kit-8; sh, short hairpin; LV, lentivirus; ns, not significant.

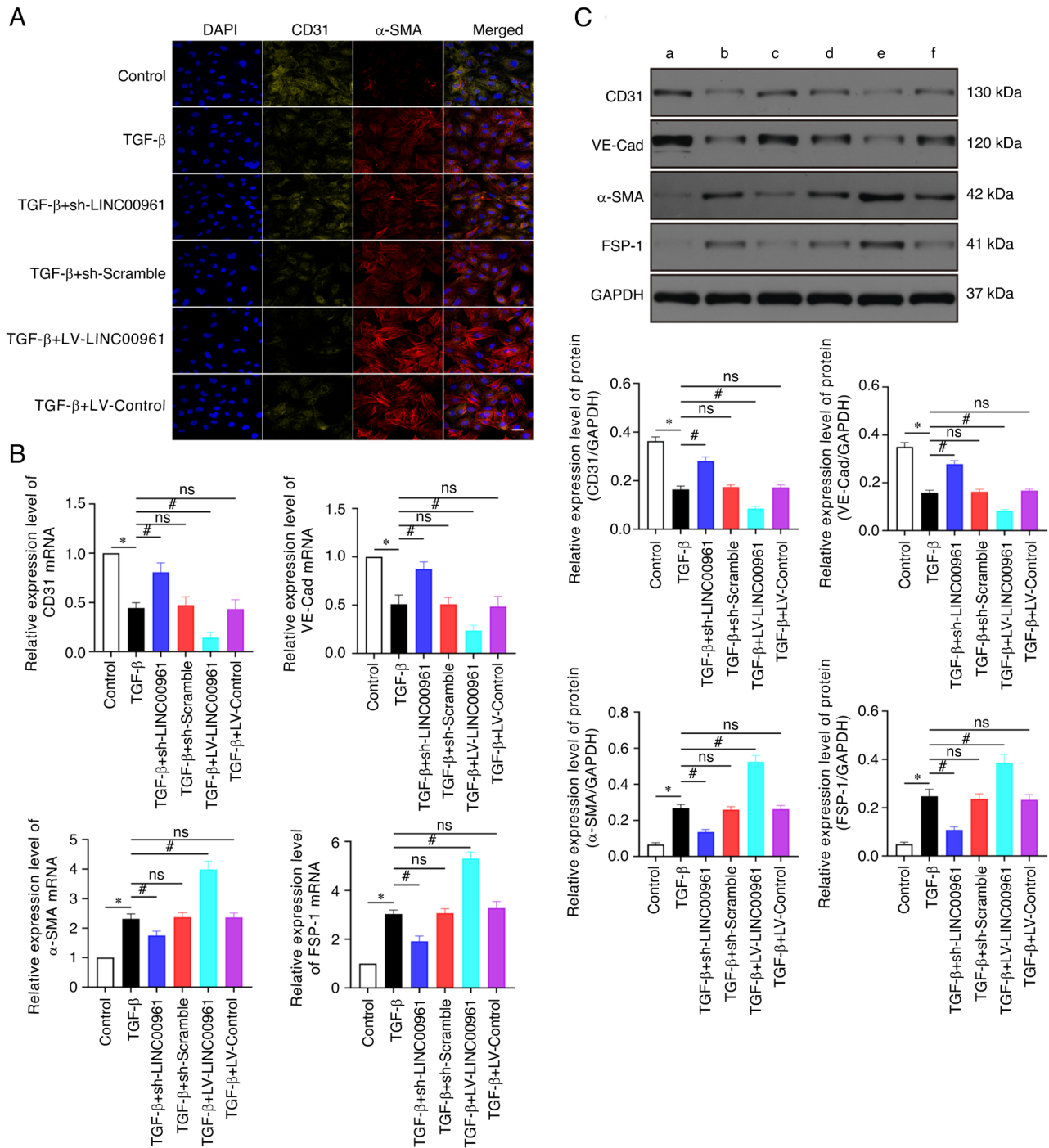


Figure 3. LINC00961 knockdown attenuates TGF- $\beta$ -induced EndMT. (A) Immunofluorescence staining was used to identify CD31<sup>+</sup>/ $\alpha$ -SMA<sup>+</sup> cells.  $\alpha$ -SMA (red), CD31 (green); scale bars: 50  $\mu$ m. (B) Reverse transcription-quantitative PCR was used to evaluate EndMT-related mRNA. (C) Western blotting was used to evaluate EndMT-related proteins. (a) Control, (b) TGF- $\beta$ , (c) TGF- $\beta$  + sh-LINC00961, (d) TGF- $\beta$  + sh-Scramble, (e) TGF- $\beta$  + LV-LINC00961 and (f) TGF- $\beta$  + LV-Control. Each experiment was repeated at least three times, ns,  $P > 0.05$ ; \* $P < 0.05$  and # $P < 0.05$ ,  $n = 5$  per group. EndMT, endothelial-mesenchymal transition;  $\alpha$ -SMA,  $\alpha$ -smooth muscle actin; sh-, short hairpin; LV, lentivirus; VE-Cad, VE cadherin; FSP-1, fibroblast specific protein 1; ns, not significant.

detect the rate of apoptosis, which showed that LINC00961 overexpression further facilitated TGF- $\beta$ -induced apoptosis. However, TGF- $\beta$ -mediated apoptosis was reduced by LINC00961 knockdown (Fig. 2D). The mRNA transcription levels of the anti-apoptotic proteins Bcl-2 and cyclin D1 were decreased by TGF- $\beta$  but were recovered when LINC00961 was knocked down, and further reduced when LINC00961 was overexpressed, whereas the mRNA transcription level of the proapoptotic protein Bax presented the opposite

trend (Fig. 2E). In addition, western blotting was performed to assess changes in protein levels of Bax, Bcl-2 and Cyclin D1. It was identified that the protein levels exhibited similar trends as those of the mRNA transcription levels (Fig. 2F). These results indicated that TGF- $\beta$ -mediated apoptosis was attenuated by LINC00961 knockdown.

*LINC00961 knockdown attenuates TGF- $\beta$ -induced EndMT.* As revealed in Fig. 3, the results of RT-qPCR and western

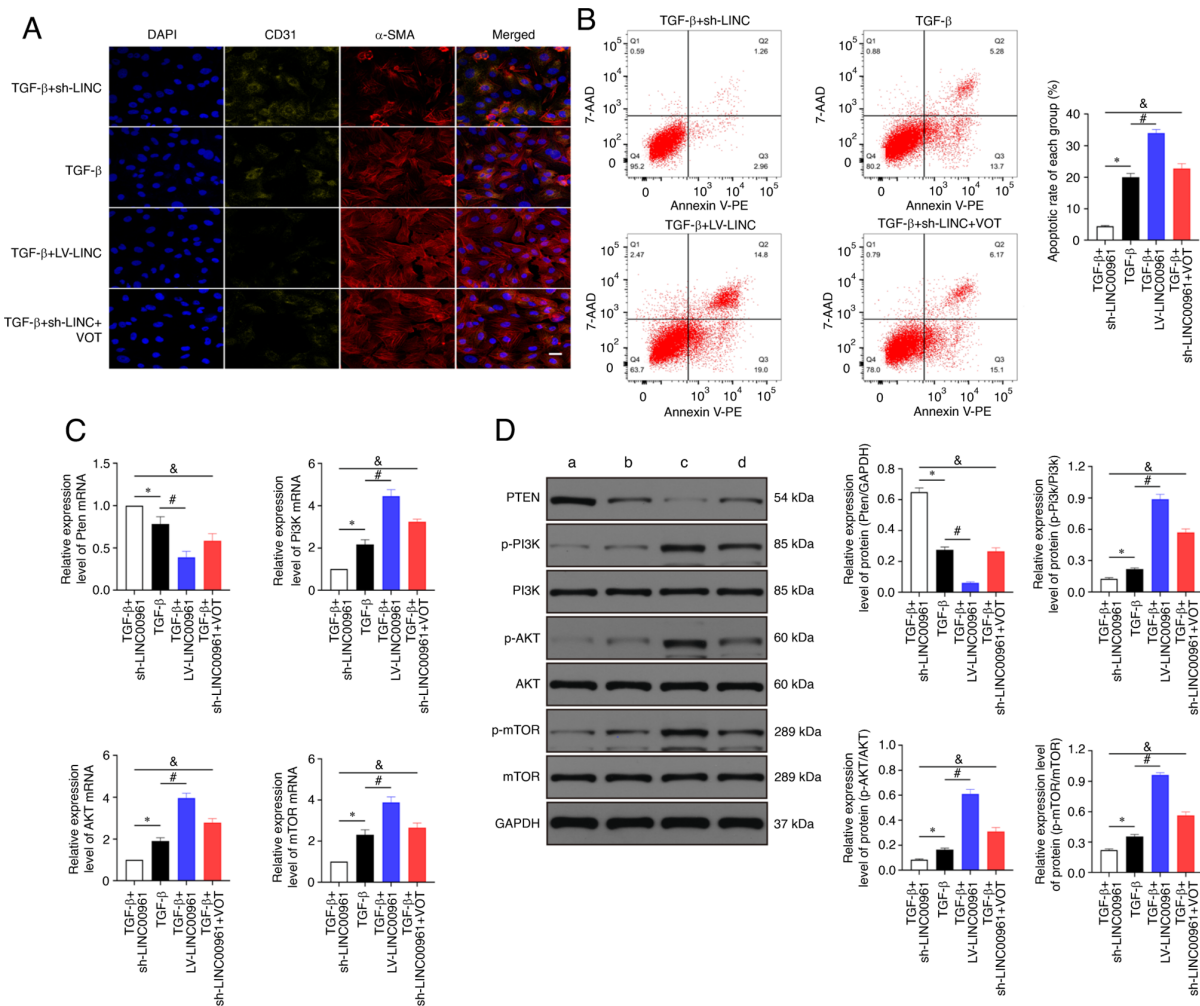


Figure 4. LINC00961 knockdown attenuates injury and EndMT in HCMECs by activating the PTEN-PI3K-AKT signalling pathway. (A) Immunofluorescence staining was used to identify CD31 + / $\alpha$ -SMA+ cells.  $\alpha$ -SMA (red), CD31 (green); scale bars: 50  $\mu$ m. (B) Rate of cell apoptosis was evaluated using flow cytometry. (C) Reverse transcription-quantitative PCR was used to determine the expression of PTEN, PI3K, AKT and mTOR mRNA. (D) Western blotting was used to determine the protein expression of PTEN, p-PI3K, PI3K, p-AKT, AKT, p-mTOR and mTOR. (a) TGF- $\beta$  + sh-LINC00961, (b) TGF- $\beta$ , (c) TGF- $\beta$  + LV-LINC00961 and (d) TGF- $\beta$  + sh-LINC00961 + VOT. Each experiment was repeated at least three times. ns,  $P > 0.05$ ; \* $P < 0.05$ , # $P < 0.05$  and & $P < 0.05$ . n=5 per group. EndMT, endothelial-mesenchymal transition; HCMECs, human cardiac microvascular endothelial cells; PTEN, phosphatase and tensin homolog deleted on chromosome 10;  $\alpha$ -SMA,  $\alpha$ -smooth muscle actin; p-, phosphorylated; sh-, short hairpin; LV, lentivirus; VOT, VO-OHpic trihydrate; ns, not significant.

blotting demonstrated that VE-Cad and CD31 expression was significantly downregulated after TGF- $\beta$  treatment compared with the control group (Fig. 3B and C;  $P < 0.05$ ). By contrast, FSP-1 and  $\alpha$ -SMA expression levels were significantly upregulated (Fig. 3B and C;  $P < 0.05$ ) in the TGF- $\beta$  group compared with those in the control group. VE-Cad and CD31 expression levels were significantly upregulated ( $P < 0.05$ ), whereas FSP-1 and  $\alpha$ -SMA expression levels were significantly downregulated ( $P < 0.05$ ) in the TGF- $\beta$  + sh-LINC00961 group compared with those in the TGF- $\beta$  group (Fig. 3B and C). The VE-cadherin and CD31 expression levels were significantly downregulated ( $P < 0.05$ ), whereas FSP-1 and  $\alpha$ -SMA levels were significantly upregulated ( $P < 0.05$ ) in the TGF- $\beta$  + LV-LINC00961 group compared with those in the TGF- $\beta$  group (Fig. 3B and C). Immunofluorescence used to assess the changes in CD31 and  $\alpha$ -SMA expression levels showed the same trends as RT-qPCR and western blotting (Fig. 3A). These data revealed that TGF- $\beta$ -induced EndMT was attenuated by LINC00961 knockdown.

*LINC00961 knockdown attenuates injury and EndMT of HCMECs by activating the PTEN-PI3K-AKT signalling pathway.* Immunofluorescence staining indicated that  $\alpha$ -SMA expression was significantly increased and CD31 expression was significantly decreased in the TGF- $\beta$  + LV-LINC00961 group compared with that in the TGF- $\beta$  group. CD31+ was significantly increased, whereas the  $\alpha$ -SMA+ level was decreased significantly in the TGF- $\beta$  + sh-LINC00961 group compared with that in the TGF- $\beta$  group. However, the expression level was reversed when the TGF- $\beta$  + sh-LINC00961 group was treated with VOT (Fig. 4A). As revealed in Fig. 4B, LINC00961 overexpression promoted cell apoptosis that had been affected by TGF- $\beta$ . LINC00961 knockdown attenuated the cell apoptosis rate that had been affected by TGF- $\beta$ ; however, the rate of cell apoptosis was reversed when the LINC00961 knockdown group was treated with VOT. The RT-qPCR results demonstrated that PTEN mRNA transcription levels were significantly reduced ( $P < 0.05$ ) and the PI3K, AKT and mTOR mRNA transcription levels were significantly

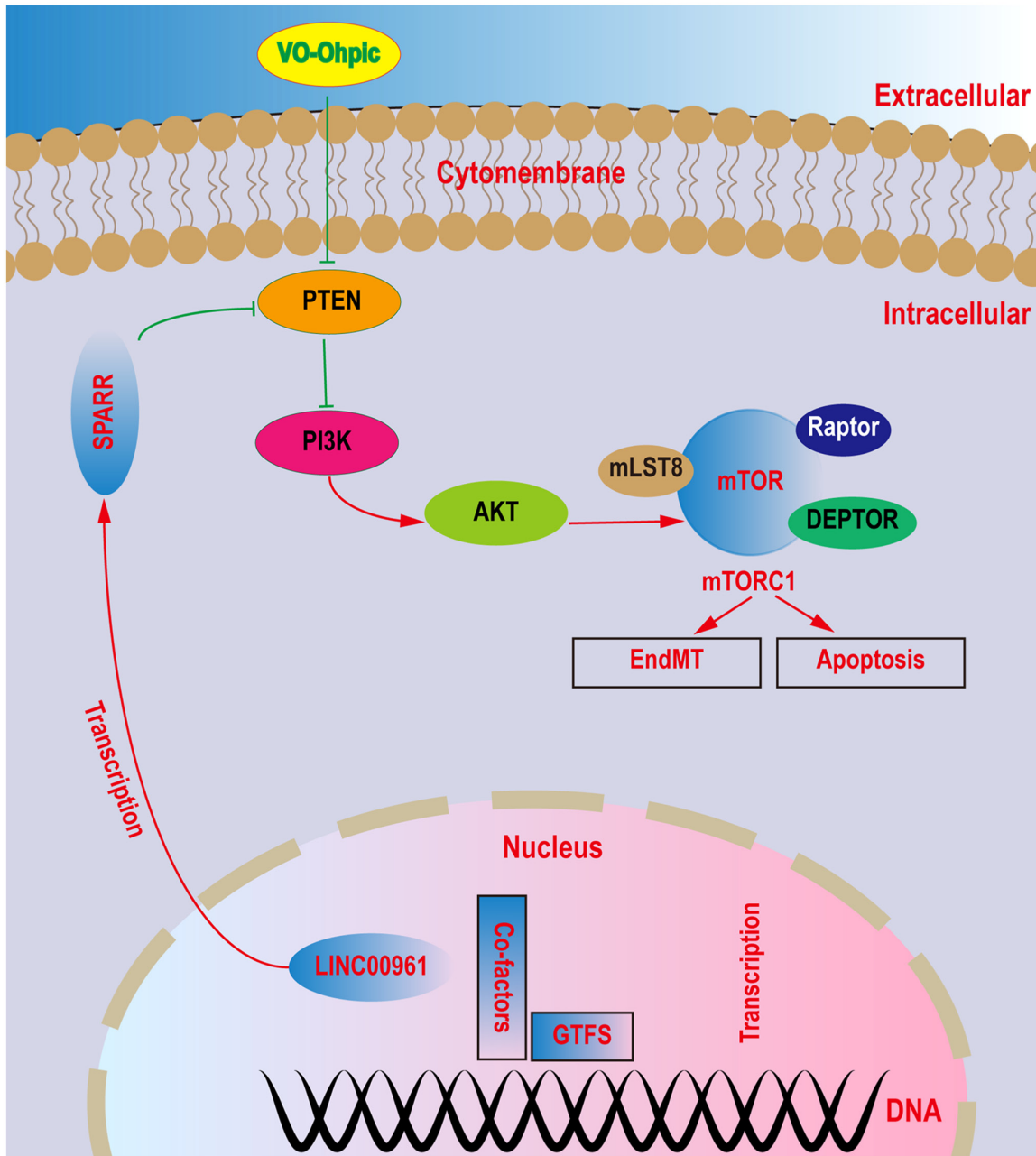


Figure 5. Schematic figure highlighting the connections among identified proteins and their roles. LINC00961 knockdown attenuates endothelial injuries and endothelial-mesenchymal transition *in vitro* by suppressing the PTEN-PI3K-AKT pathway.

increased ( $P < 0.05$ ) in the TGF- $\beta$  + LV-LINC00961 group compared with those in the TGF- $\beta$  group (Fig. 4C). The RT-qPCR results also indicated that the PTEN mRNA transcription level was decreased and PI3K, AKT and mTOR mRNA transcription levels were reduced ( $P < 0.05$ ) in the TGF- $\beta$  + sh-LINC00961 group compared with those in the TGF- $\beta$  group. However, these mRNA transcription levels were reversed when the TGF- $\beta$  + sh-LINC00961 group was treated with VOT. In addition, western blotting was performed to examine changes in protein levels (Fig. 4D). According to the aforementioned data, LINC00961 knockdown by TGF- $\beta$  induced injury and EndMT in HCMECs, possibly through activation of PTEN and inhibition of PI3K, AKT, and mTOR. The relationships among these proteins are schematically represented in Fig. 5.

## Discussion

HCMECs play crucial physiological roles in maintaining the normal function of the heart, and their dysfunction leads to various cardiovascular diseases, such as ischemic cardiomyopathy, diabetic cardiomyopathy, myocardial infarction and heart failure (30-32). Human umbilical vein endothelial cells and human coronary artery endothelial cells have been used to investigate EndMT (33). To meet physiological requirements *in vivo*, HCMECs were used to evaluate EndMT. EndMT can be induced by TGF- $\beta$  and hypoxia in HCMECs, and certain studies (18,34) showed that hypoxia can activate autophagy; therefore, TGF- $\beta$  was used to induce EndMT to avoid the effect of autophagy.

LncRNAs are associated with a range of cellular biological functions, such as RNA splicing, protein

localisation and chromatin modification (35,36). Previously, Matsumoto *et al* (37) reported that LINC00961 generated SPAR polypeptide that acted via the lysosome to suppress amino-acid-mediated mTORC1 activity, thereby modulating skeletal muscle regenerative response following injury. Since their discovery, lncRNAs had reshaped our thinking on the design and regulatory landscape of genomes in metazoans. LncRNAs bear some of the hallmarks of mRNAs, as they are transcribed by RNA polymerase II, spliced, capped, and polyadenylated, yet they have been initially surmised to have little to no ORF information. LncRNAs were generally less widely expressed than mRNAs, thus raising the notion that they actively regulated specific biological processes (37). The efficacy of LINC00961 in inhibiting tumour growth, invasion and metastasis and regulating endothelial cell function has been extensively examined (9,38,39). The role of lncRNA LINC00961 has also gained attention in cardiovascular diseases (12,40,41). Based on the relationship between LINC00961 and cardiovascular diseases, the effect of this lncRNA on EndMT was examined *in vitro* and its underlying mechanisms were investigated.

During EndMT, the expression of related proteins is altered, including increased FSP-1 and SMA and decreased CD31 and VE-Cad (42). It was found that the protein expression of BAX, caspase,  $\alpha$ -SMA and FSP-1 was increased, whereas that of Bcl-2, cyclin D1, CD31 and VE-cadherin was decreased in endothelial cells treated with TGF- $\beta$ . LINC00961 knockdown reversed these alterations.

The PTEN inhibitor VOT was used to explore the underlying mechanism of LINC00961 in EndMT and cell injuries. LINC00961 knockdown downregulated the protein levels of p-PI3K, p-AKT, and p-mTOR and upregulated the protein level of PTEN. When PTEN was inhibited using VOT, the effects of LINC00961 knockdown on p-PI3K, p-AKT and p-mTOR were diminished. Based on these results, LINC00961 knockdown attenuated TGF- $\beta$ -induced EndMT and cell injuries by activating the PTEN-PI3K-AKT pathway, which is consistent with the results of previous studies. For example, LINC00961 downregulation promotes the proliferation and inhibits the apoptosis of vascular smooth muscle cells (12). Liu *et al* (11) revealed that LINC00961 promoted myocardial infarction in the myocardial cell line H9c2. Considering the association of the PTEN-PI3K-AKT pathway with EndMT, LINC00961 has been considered as a diagnostic target to promote EndMT and myocardial fibrosis. In summary, LINC00961 knockdown attenuated endothelial cell injury and EndMT induced by TGF- $\beta$  via the PTEN-PI3K-AKT signalling pathway. To confirm our results, further studies are needed to investigate the effects of LINC00961 in animal models and other cell lines (such as cardiomyocytes and fibroblasts). Additionally, other proteins related to the PTEN-PI3K-AKT pathway and EndMT and further methods should be used, including a luciferase assay.

In conclusion, it was revealed that LINC00961 knockdown attenuates injuries and EndMT in HCMECs *in vitro* by activating PTEN expression and inhibiting PI3K, AKT and mTOR expression. Inhibition of LINC00961 expression may prevent the occurrence of EndMT-related cardiovascular diseases, such as myocardial fibrosis and heart failure, and shows potential as a therapeutic target for cardiovascular diseases.

## Acknowledgements

Not applicable.

## Funding

The present study was supported by the Youth Project of Jiangxi Provincial Education Department Project (grant no. GJJ190129) and the National Natural Science Foundation of China.

## Availability of data and materials

The datasets used and/or analyzed during the current study are available from the corresponding author on reasonable request.

## Authors' contributions

JXH performed the high-throughput sequencing experiments and the bioinformatics analysis. BGL, ZQZ, TK, WQ and SHH performed the histological examination of the kidney, and were major contributors in writing the manuscript. JXH and BGL confirm the authenticity of all the raw data. All authors read and approved the final manuscript.

## Ethics approval and consent to participate

Animal experiments were approved by the Laboratory Animal Ethics Committee of the First Affiliated Hospital of Nanchang University (Nanchang, China; approval no. 20210213).

## Patient consent for publication

Not applicable.

## Competing interests

The authors declare that they have no competing interests.

## References

1. Talman V and Ruskoaho H: Cardiac fibrosis in myocardial infarction—from repair and remodeling to regeneration. *Cell Tissue Res* 365: 563-581, 2016.
2. Vaskova E, Ikeda G, Tada Y, Wahlquist C, Mercola M and Yang PC: Sacubitril/valsartan improves cardiac function and decreases myocardial fibrosis via downregulation of exosomal miR-181a in a rodent chronic myocardial infarction model. *J Am Heart Assoc* 9: e015640, 2020.
3. Liu W, Sun J, Guo Y, Liu N, Ding X, Zhang X, Chi J, Kang N, Liu Y and Yin X: Calhex231 ameliorates myocardial fibrosis post myocardial infarction in rats through the autophagy-NLRP3 inflammasome pathway in macrophages. *J Cell Mol Med* 24: 13440-13453, 2020.
4. Chi YC, Shi CL, Zhou M, Liu Y, Zhang G and Hou SA: Selective cyclooxygenase-2 inhibitor NS-398 attenuates myocardial fibrosis in mice after myocardial infarction via snail signaling pathway. *Eur Rev Med Pharmacol Sci* 21: 5805-5812, 2017.
5. Shibamoto M, Higo T, Naito AT, Nakagawa A, Sumida T, Okada K, Sakai T, Kuramoto Y, Yamaguchi T, Ito M, *et al*: Activation of DNA damage response and cellular senescence in cardiac fibroblasts limit cardiac fibrosis after myocardial infarction. *Int Heart J* 60: 944-957, 2019.
6. Tajbakhsh S: lncRNA-encoded polypeptide SPAR(s) with mTORC1 to regulate skeletal muscle regeneration. *Cell Stem Cell* 20: 428-430, 2017.

7. Mu X, Mou KH, Ge R, Han D, Zhou Y and Wang LJ: Linc00961 inhibits the proliferation and invasion of skin melanoma by targeting the miR367/PTEN axis. *Int J Oncol* 55: 708-720, 2019.
8. Wu H, Dai Y, Zhang D, Zhang X, He Z, Xie X and Cai C: LINC00961 inhibits the migration and invasion of colon cancer cells by sponging miR-223-3p and targeting SOX11. *Cancer Med* 9: 2514-2523, 2020.
9. Zhang L, Shao L and Hu Y: Long noncoding RNA LINC00961 inhibited cell proliferation and invasion through regulating the Wnt/beta-catenin signaling pathway in tongue squamous cell carcinoma. *J Cell Biochem* 120: 12429-12435, 2019.
10. Spencer HL, Sanders R, Boulberdaa M, Meloni M, Cochrane A, Spiroski AM, Mountford J, Emanuelli C, Caporali A, Brittan M, *et al*: The LINC00961 transcript and its encoded micropeptide SPAAR regulate endothelial cell function. *Cardiovasc Res* 116: 1981-1994, 2020.
11. Liu S, He Y, Shi J, Liu L, Ma H, He L and Guo Y: STAT1-activated LINC00961 regulates myocardial infarction by the PI3K/AKT/GSK3 $\beta$  signaling pathway. *J Cell Biochem* 120: 13226-13236, 2019.
12. Wu CT, Liu S and Tang M: Downregulation of linc00961 contributes to promote proliferation and inhibit apoptosis of vascular smooth muscle cell by sponging miR-367 in patients with coronary heart disease. *Eur Rev Med Pharmacol Sci* 23: 8540-8550, 2019.
13. Markwald RR, Fitzharris TP and Smith WN: Structural analysis of endocardial cytodifferentiation. *Dev Biol* 42: 160-180, 1975.
14. Liu X, Mujahid H, Rong B, Lu QH, Zhang W, Li P, Li N, Liang ES, Wang Q, Tang DQ, *et al*: Irisin inhibits high glucose-induced endothelial-to-mesenchymal transition and exerts a dose-dependent bidirectional effect on diabetic cardiomyopathy. *J Cell Mol Med* 22: 808-822, 2018.
15. Feng B, Cao Y, Chen S, Chu X, Chu Y and Chakrabarti S: miR-200b mediates endothelial-to-mesenchymal transition in diabetic cardiomyopathy. *Diabetes* 65: 768-779, 2016.
16. Yin Y, Zhang Q, Zhao Q, Ding G, Wei C, Chang L, Li H, Bei H, Wang H, Liang J and Jia Z: Tongxinluo attenuates myocardial fibrosis after acute myocardial infarction in rats via inhibition of endothelial-to-mesenchymal transition. *BioMed Res Int* 16: 6595437, 2019.
17. Zheng X, Peng M, Li Y, Wang X, Lu W, Wang X, Shan Y, Li R, Gao L and Qiu C: Cathelicidin-related antimicrobial peptide protects against cardiac fibrosis in diabetic mice heart by regulating endothelial-mesenchymal transition. *Int J Biol Sci* 15: 2393-2407, 2019.
18. Zou J, Liu Y, Li B, Zheng Z, Ke X, Hao Y, Li X, Li X, Liu F and Zhang Z: Autophagy attenuates endothelial-to-mesenchymal transition by promoting snail degradation in human cardiac microvascular endothelial cells. *Biosci Rep* 37: BSR20171049, 2017.
19. Liu Y, Zou J, Li B, Wang Y, Wang D, Hao Y, Ke X and Li X: RUNX3 modulates hypoxia-induced endothelial-to-mesenchymal transition of human cardiac microvascular endothelial cells. *Int J Mol Med* 40: 65-74, 2017.
20. Hu J, Zheng Z, Li X, Li B, Lai X, Li N and Lei S: Metformin attenuates hypoxia-induced endothelial cell injury by activating the AMP-activated protein kinase pathway. *J Cardiovasc Pharmacol* 77: 862-874, 2021.
21. Gao X, Qin T, Mao J, Zhang J, Fan S, Lu Y, Sun Z, Zhang Q, Song B and Li L: PTEN/miR-20a/PTEN axis contributes to breast cancer progression by regulating PTEN via PI3K/AKT pathway. *J Exp Clin Cancer Res* 38: 256, 2019.
22. Chai C, Song LJ, Han SY, Li XQ and Li M: MicroRNA-21 promotes glioma cell proliferation and inhibits senescence and apoptosis by targeting SPRY1 via the PTEN/PI3K/AKT signaling pathway. *CNS Neurosci Ther* 24: 369-380, 2018.
23. Hervera A, De Virgiliis F, Palmisano I, Zhou L, Tantardini E, Kong G, Hutson T, Danzi MC, Perry RB, Santos CX, *et al*: Reactive oxygen species regulate axonal regeneration through the release of exosomal NADPH oxidase 2 complexes into injured axons. *Nat Cell Biol* 20: 307-319, 2018.
24. Cheng S, Zhang X, Feng Q, Chen J, Shen L, Yu P, Yang L, Chen D, Zhang H, Sun W and Chen X: Astragaloside IV exerts angiogenesis and cardioprotection after myocardial infarction via regulating PTEN/PI3K/Akt signaling pathway. *Life Sci* 227: 82-93, 2019.
25. Cao L, Graue-Hernandez EO, Tran V, Reid B, Pu J, Mannis MJ and Zhao M: Downregulation of PTEN at corneal wound sites accelerates wound healing through increased cell migration. *Invest Ophthalmol Vis Sci* 52: 2272-2278, 2011.
26. Yang W, Wu Z, Yang K, Han Y, Chen Y, Zhao W, Huang F, Jin Y and Jin W: BMI1 promotes cardiac fibrosis in ischemia-induced heart failure via the PTEN-PI3K/Akt-mTOR signaling pathway. *Am J Physiol Heart Circ Physiol* 316: H61-H69, 2019.
27. Zhang M, Weng H and Zheng J: NAD(+) repletion inhibits the endothelial-to-mesenchymal transition induced by TGF- $\beta$  in endothelial cells through improving mitochondrial unfolded protein response. *Int J Biochem Cell Biol* 117: 105635, 2019.
28. Zonghai C, Tao L, Pengjiao M, Liang G, Rongchuan Z, Xinyan W, Wenyi N, Wei L, Yi W and Lang B: Mycobacterium tuberculosis ESAT6 modulates host innate immunity by downregulating miR-222-3p target PTEN. *Biochim Biophys Acta Mol Basis Dis* 1868: 166292, 2022.
29. Livak KJ and Schmittgen TD: Analysis of relative gene expression data using real-time quantitative PCR and the 2(-Delta Delta C(T)) method. *Methods* 25: 402-408, 2001.
30. Lei W, Li J, Li C, Chen L, Huang F, Xiao D, Zhang J, Zhao J, Li G, Qu T, *et al*: MARCH5 restores endothelial cell function against ischaemic/hypoxia injury via Akt/eNOS pathway. *J Cell Mol Med* 25: 3182-3193, 2021.
31. Feng B, Chen S, Gordon AD and Chakrabarti S: miR-146a mediates inflammatory changes and fibrosis in the heart in diabetes. *J Mol Cell Cardiol* 105: 70-76, 2017.
32. Quan X, Liu X, Qin X, Wang Y, Sun T, Li Z, Zhu L, Chen J, Zhou Y, Singh S, *et al*: The role of LR-TIMAP/PP1c complex in the occurrence and development of no-reflow. *EBioMedicine* 65: 103251, 2021.
33. Tian J, Zhang M, Suo M, Liu D, Wang X, Liu M, Pan J, Jin T and An F: Dapagliflozin alleviates cardiac fibrosis through suppressing EndMT and fibroblast activation via AMPK $\alpha$ /TGF- $\beta$ /Smad signalling in type 2 diabetic rats. *J Cell Mol Med* 25: 7642-7659, 2021.
34. Qureshi-Baig K, Kuhn D, Viry E, Pozdeev VI, Schmitz M, Rodriguez F, Ullmann P, Koncina E, Nurmik M, Frasilho S, *et al*: Hypoxia-induced autophagy drives colorectal cancer initiation and progression by activating the PRKC/PKC-EZR (ezrin) pathway. *Autophagy* 16: 1436-1452, 2020.
35. Geisler S and Coller J: RNA in unexpected places: Long non-coding RNA functions in diverse cellular contexts. *Nat Rev Mol Cell Biol* 14: 699-712, 2013.
36. Matkovich SJ, Edwards JR, Grossenheider TC, de Guzman Strong C and Dorn GW II: Epigenetic coordination of embryonic heart transcription by dynamically regulated long noncoding RNAs. *Proc Natl Acad Sci USA* 111: 12264-12269, 2014.
37. Matsumoto A, Pasut A, Matsumoto M, Yamashita R, Fung J, Monteleone E, Saghatelian A, Nakayama KI, Clohessy JG and Pandolfi PP: mTORC1 and muscle regeneration are regulated by the LINC00961-encoded SPAR polypeptide. *Nature* 541: 228-232, 2017.
38. Pan LN and Sun YR: LINC00961 suppresses cell proliferation and induces cell apoptosis in oral squamous cell carcinoma. *Eur Rev Med Pharmacol Sci* 23: 3358-3365, 2019.
39. Chen D, Zhu M, Su H, Chen J, Xu X and Cao C: LINC00961 restrains cancer progression via modulating epithelial-mesenchymal transition in renal cell carcinoma. *J Cell Physiol* 234: 7257-7265, 2019.
40. Spiroski AM, Sanders R, Meloni M, McCracken IR, Thomson A, Brittan M, Gray GA and Baker AH: The influence of the LINC00961/SPAAR locus loss on murine development, myocardial dynamics, and cardiac response to myocardial infarction. *Int J Mol Sci* 22: 969, 2021.
41. Yin J, Liu Q, Chen C and Liu W: Small regulatory polypeptide of amino acid response negatively relates to poor prognosis and controls hepatocellular carcinoma progression via regulating microRNA-5581-3p/human cardiolipin synthase 1. *J Cell Physiol* 234: 17589-17599, 2019.
42. Piera-Velazquez S, Li Z and Jimenez SA: Role of endothelial-mesenchymal transition (EndMT) in the pathogenesis of fibrotic disorders. *Am J Pathol* 179: 1074-1080, 2011.



This work is licensed under a Creative Commons Attribution-NonCommercial-NoDerivatives 4.0 International (CC BY-NC-ND 4.0) License.